minerals

MDPI

Review

Towards a Mineral Systems Model for Surficial Uranium Mineralization Based on Deposits in the Erongo District of Namibia

Andy Wilde

Centre for Exploration Targeting (CET), The University of Western Australia, 35 Stirling Highway, Crawley, WA 6009, Australia; wildegeoscience@gmail.com

Abstract: Surficial deposits in Namibia's Erongo district contain substantial but low-grade resources of uranium and vanadium (nearly 500 Mlb U_3O_8), hosted in palaeochannels. This review attempts to develop a mineral systems model for the deposit type, but it is emphasised that research into this important class of deposit has been minimal since the nineteen eighties, largely as a result of a limited investment in uranium exploration. The deposits are the result of groundwater movement in aquifers developed within Cenozoic palaeochannels. The source of uranium was probably granitic rocks traversed by these palaeodrainages, particularly black-quartz rich pegmatites similar to those that make up the hard-rock alaskite deposits of the region. Transport of uranium is generally assumed to have occurred in aqueous uranium species after palaeochannels became filled with sediment. U-enriched clasts within the palaeochannels have yet to be investigated as a local source of uranium. The localised deposition of uranium occurred after regionally extensive carbonate cementation of the palaeochannel sediments, which was the result of climate change (aridification). Pre-uranium calcite may have acted as a chemical buffer (pH) and probably influenced palaeochannel hydrology, restricting groundwater flow to the deeper portions. Uranium is paragenetically related to Mg clays and dolomite, suggesting that the groundwater evolved to a more Mg-rich composition during uranium deposition, probably as a result of more extreme evaporation. The controls on the localisation of mineralisation remain unclear and unpredictable, as are the controls on uranium grade—the fundamental determinant of economic viability. There are few absolute age determinations for any of the deposits, but none occur in rocks likely to be older than the Miocene. This reflects low preservation potential. For example, the Langer Heinrich deposit is incised by active drainage with attendant erosion and probable removal of mineralised material.

Keywords: uranium; surficial; mineral systems analysis; Erongo district; Namibia

Citation: Wilde, A. Towards a Mineral Systems Model for Surficial Uranium Mineralization Based on Deposits in the Erongo District of Namibia. *Minerals* **2023**, *13*, 149. https://doi.org/10.3390/min13020149

Academic Editor: Massimo D'Antonio

Received: 21 December 2022
Revised: 5 January 2023
Accepted: 17 January 2023
Published: 19 January 2023

1. Introduction

Growing demand for green energy is manifested in a large number of nuclear reactors both planned under construction. This increase in global nuclear capacity will require the discovery of additional uranium resources to meet the increased demand for and decreasing supply of uranium. In this paper, the surficial type (also known as the calcrete- or palaeochannel-hosted type [1]) of uranium deposit is reviewed with a view to developing a mineral systems model that might aid in future exploration. As with many types of uranium deposit, research on surficial uranium deposits has been negligible in recent years, reflecting a past oversupply of uranium and a reduced investment in uranium exploration. It is hoped that this review might stimulate new research to help discover new examples of this deposit type.

Numerous examples of surficial uranium deposits occur on many continents, but the most widely documented and largest deposits occur in Namibia, Australia and Jordan. This review is confined to the Namibian deposits, which, as will be shown below, are probably fossil deposits and, as such, differ from Australian deposits, which are probably

still forming [2]. In the first part of this review, background and descriptive information are presented for the deposits. In the discussion section, key features of the deposits are discussed in the context of the mineral systems approach [3–5].

Namibia's Erongo region contains sixteen surficial uranium–vanadium deposits and several occurrences hosted within unmetamorphosed sediments that fill palaeochannels, developed on Proterozoic and Early Palaeozoic (Damaran) metamorphic and igneous basement rocks. The contained uranium resource of these deposits amounts to nearly half a billion pounds of U_3O_8, making this region the best-endowed region in the world for this type of deposit (Table 1). Uranium grades are low ranging, from 80 to 540 ppm U_3O_8 (Table 1).

Table 1. Uranium resources of palaeochannel type deposits in the Erongo region of Namibia [6–8].

Deposit Name	Ore (Mt)	Grade (ppm U_3O_8)	Contained U_3O_8 (Mlb)
Langer Heinrich	145.9	535	171.9
Tumas 1, 2 and 3	200.0	258	114.1
Klein Trekkopje	25.0	105	57.9
Marenica	276.0	94	57.3
Aussinanis	34.6	237	18.0
Koppies (Tumas)	37.1	208	17.0
Trekkopje	46.0	129	13.1
Tubas Red Sand	34.0	170	12.7
Klein Spitzkoppe	25.0	150	11.2
Welwitschia Flats	35.0	120	9.2
Tubas Calcrete	7.4	374	6.1
MA 7	22.8	80	4.1
Brandberg	3.0	212	1.4
Hakskeen	0.4	331	0.3
TOTAL	855.0		494.3

The term "calcrete" is used extensively in this paper. There is no universally accepted definition of the term, which is synonymous with kankar, kunkar, caliche and others [9]. There is no strict definition of the amount of carbonate minerals that must be present in order for the rock to qualify as a calcrete. Informally, a calcrete should contain over 40% carbonate [9], but the amount of carbonate is seldom accurately determined. The usage below is adopted from the various source publications.

Mineral Systems Approach to Predictive Exploration

The Mineral Systems Approach considers the origin of mineral deposits in the framework of lithospheric-scale processes from the time-honoured perspective of source, fluids, transport and traps. Applied to exploration strategy, this approach allows for more predictive models. Rather than matching patterns, knowledge of the underlying geological processes and tectonic setting can be used to assess prospectivity. Furthermore, a Mineral Systems Approach can broaden the scope of prospectivity indicators and, therefore, can allow for earlier, more efficient fertility assessments [5,10].

The Mineral Systems Approach can be broken down into five questions; these are geodynamic history and setting, architecture, fluid reservoirs, fluid pathways, and driving forces for transport and deposition. The questions were formulated for hydrothermal mineral systems but are equally applicable to surficial uranium deposits. Translating this theory into a useful tool for exploration involves understanding how critical processes of the mineral system are reflected in the geology and how they are used to define targeting criteria to detect elements directly or by proxy [5,10].

2. Geological Setting

2.1. Namib Unconformity Surface (NUS)

Palaeochannels that host Namibia's surficial uranium deposits are developed on a basement of various igneous and metamorphic rocks of the ca 540 Ma Damaran orogen [11,12]. Protracted erosion of the orogen during the Late Cretaceous resulted in the development of a prominent palaeosurface, referred to as the Namib Unconformity Surface [13]. The

morphology of this surface and the extent to which it has been modified (incised) during later erosional and tectonic events remains uncertain, although the palaeochannels themselves have been reasonably well defined by a combination of airborne electro-magnetic surveys and drilling by several exploration companies since the 1970s (Figures 1 and 2). The palaeochannels are generally oriented NE–SW and are probably drained via outcropping basement rocks to the E and NE (Figure 1).

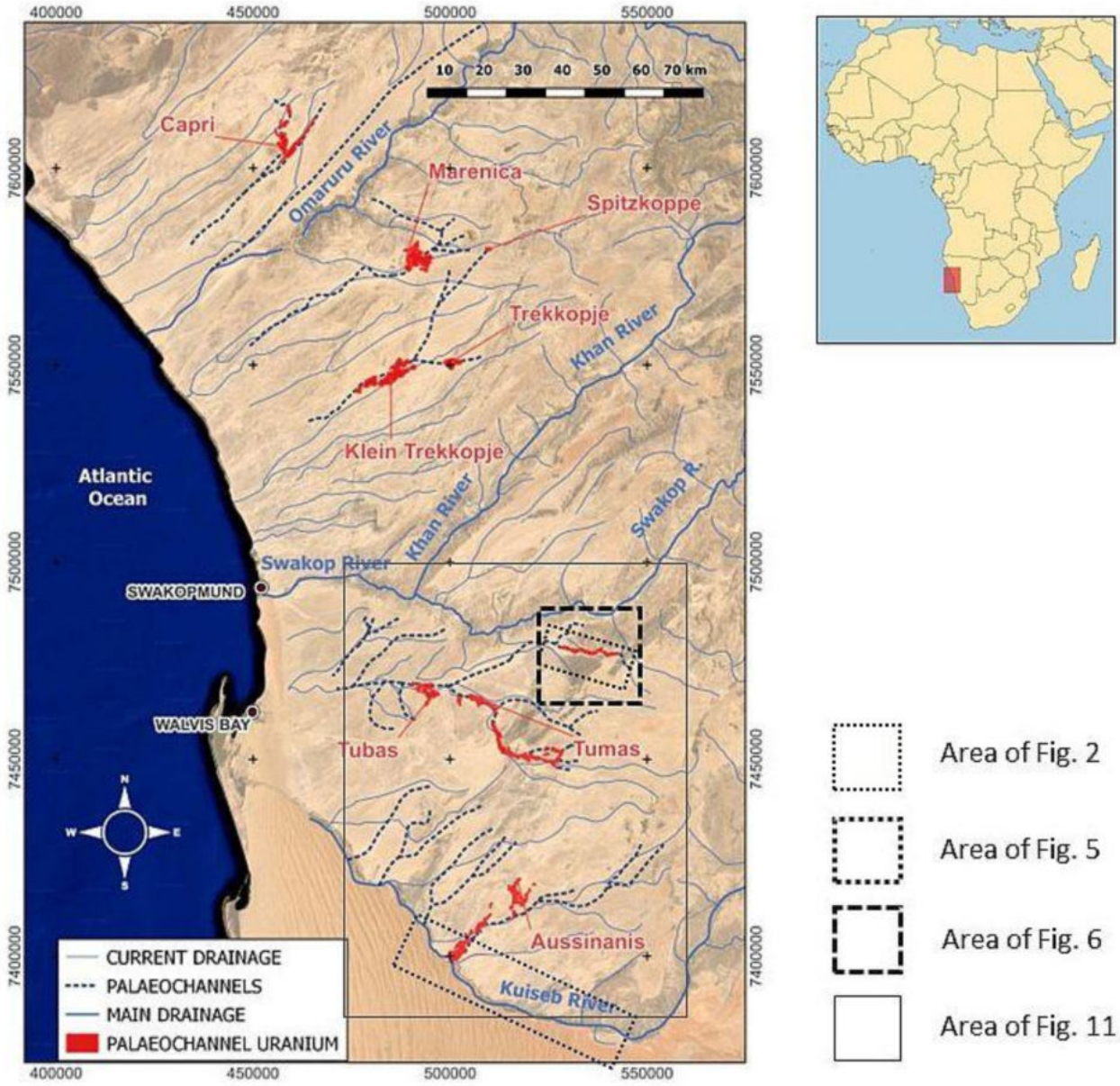

Figure 1. Location of palaeochannel-hosted uranium deposits of the Erongo region of Namibia.

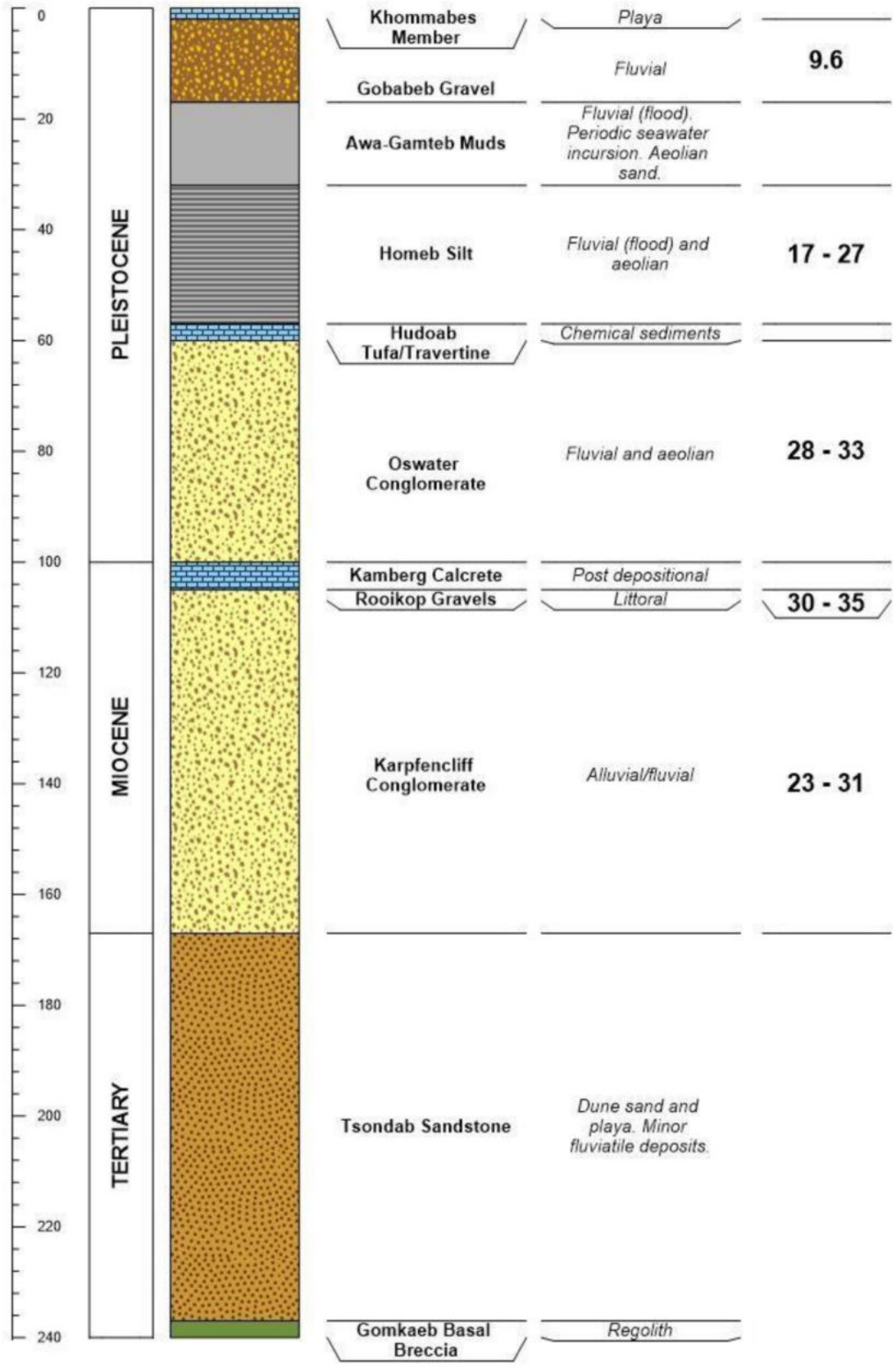

Figure 2. Stratigraphy of the Kuiseb Valley based on outcrop locations, as shown in Figure 1. Mainly after [14]. Figures to right are ^{14}C age ranges in Ka. Sources in text.

2.2. Basement Rocks & Weathering

The lithologies of Damaran basement rocks, traversed by mineralised palaeochannels, are quite varied and include gneisses, marbles, skarns and multiple generations of felsic intrusions, along with prominent Karoo-aged dolerite dykes, typically oriented north–south. The latter outcrop is rather better than the older lithologies and may have formed resistant ridge-like outcrops along the floors of the palaeochannels [15].

There is little evidence of substantial weathering in the basement rocks below the NUS, probably as a consequence of predominantly arid conditions during and since the Cretaceous period [14]. Alternatively, weathered rocks may have been partially to completely stripped during the erosive event that formed the NUS. A breccia of angular quartz vein fragments up to 3 m thick (Gomkaeb Conglomerate or basal breccia) occurs at the basement contact along the Kuiseb River and has been interpreted as a palaeoregolith [14]. Dating of the weathering-related secondary minerals at the Skorpion and Wolkenhauben base-metal deposits (to the north of the area of interest) indicates that there was at least some localised chemical weathering (and therefore a relatively humid climate) during the Late Cretaceous period, between 50 and 85 Ma [16].

2.3. Palaeovalley Fill of the Kuiseb Valley and Elsewhere

Approximately 240 m of Miocene (23 to 5.3 Ma) to Pleistocene (2.6–0.01 Ma) sediments are exposed on the flanks of the Kuiseb valley and represent erosional remnants of a sedimentary sequence that probably once filled the valley (Figure 2) [14]. The oldest unit, which directly overlies the possible regolith of the Gomakaeb basal breccia, is the Tsondab Sandstone (Figure 2). The Tsondab Sandstone is largely of aeolian origin, but contains layers of dolomite, halite, sylvite and gypsum deposited in playa lakes [14].

The deposition of the overlying Karpfenkliff Conglomerate probably reflects a change in the climate, with increased rainfall permitting the deposition of coarse fluvial debris in the ancestral Kuiseb River [14]. A prominent unconformity at the top of the Karpfenkliff Conglomerate is indicative of a neotectonic event at this time, which rejuvenated the Kuiseb River and resulted in its incision into the Miocene rocks [14].

The Pleistocene Oswater Conglomerate unconformably overlies these older rocks and in places rests directly on basement rocks. Incision by the Gawib River into the palaeochannel sediments of the Langer Heinrich deposit and diversion of the Gawib River to the north may have occurred at this time [15]. Figure 3 shows the relationship of the current ephemeral drainage of the Gawib to the remnant calcretised conglomerate.

Overlying the Oswater Conglomerate is approximately 40 m of silt and clay of the Homeb Silt, interpreted as the product of periodic flooding, indicating a return to wetter climates and also a periodic incursion by seawater [14]. The sequence is completed by recent fluvial gravels and carbonate deposits of present-day interdunal regions.

2.4. Carbonate Cementation, Tufa, Travertine and Sinter

Carbonate cementation is common throughout the Cenozoic sequence but is particularly intense in the 5-m-thick Kamberg Calcrete, which forms prominent scarps along the present-day Kuiseb valley. The Kamberg Calcrete appears to be developed mainly (though not exclusively) at the top of the Karpfenkliff Conglomerate and is regarded as a stratigraphic marker [14]. The basal contact is gradational as the calcrete grades downwards into weakly cemented conglomerate. The prominent scarp deposits, immediately to the east of the Langer Heinrich, may correlate with the Kamberg Calcrete (Figure 3A).

Carbonate cementation of the upper part of the Karpfenkliff Conglomerate must have occurred prior to the deposition of the Oswater Conglomerate, since the latter unit contains clasts of calcrete [14]. The Oswater Conglomerate is also cemented by carbonate, suggesting that there were at least two carbonate-cementing events, one of which occurred during the Miocene or Pliocene, and the other during the Pleistocene or more recently.

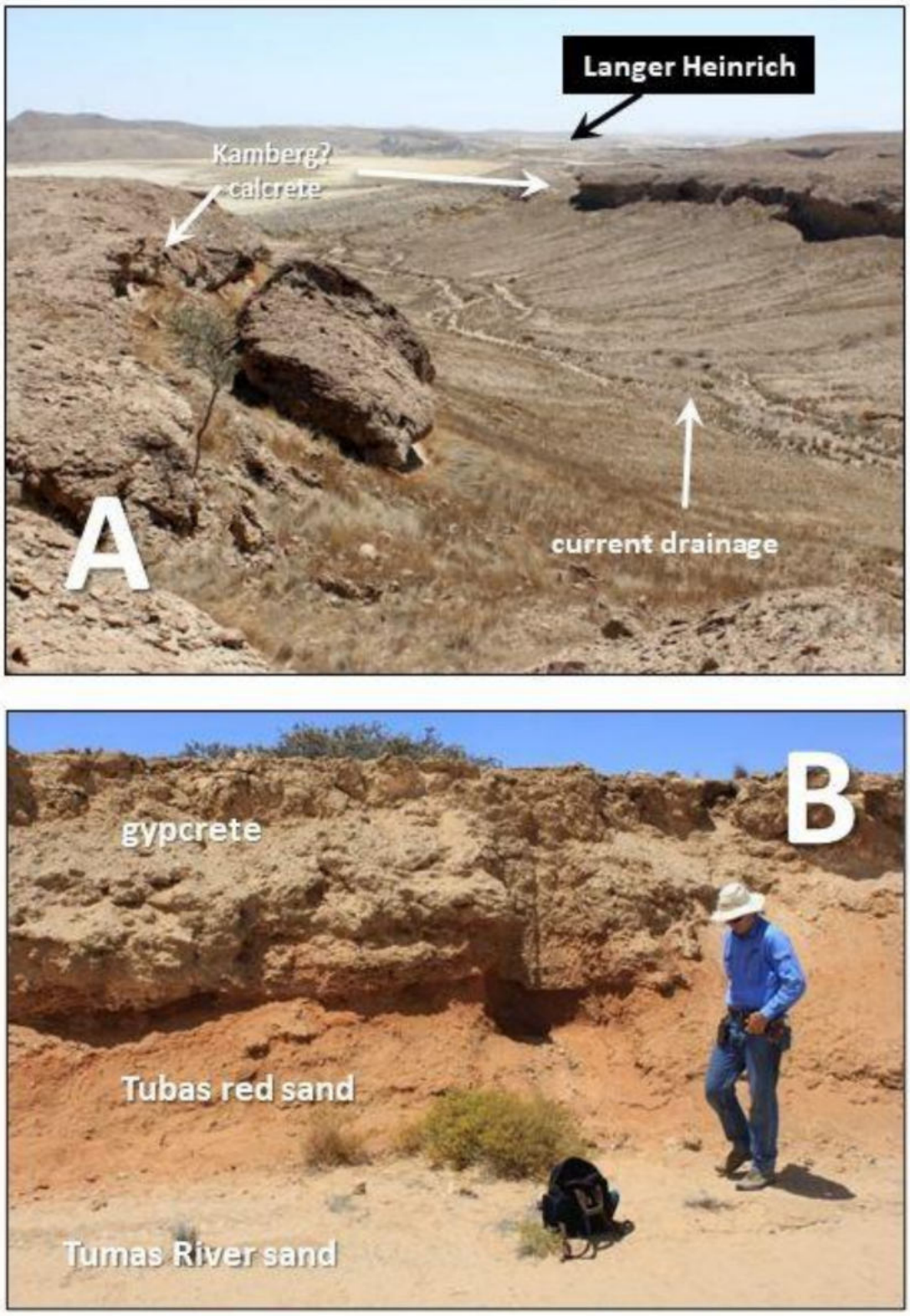

Figure 3. (**A**)—Looking westwards down the Langer Heinrich Valley showing relict calcrete deposits above the present level of the Gawib River and the uranium deposits. Hills in distance are formed by outcrops of Tinkas Formation schist. (**B**)—Rare outcrop of Tubas Red Sand overlain by gypcrete at the Tumas River. The scarp in this image is due to incision by the active Tumas River and shows that the gypcrete formation predates the Tumas River.

Carbonate cements from various stratigraphic levels have been dated using the ^{14}C method at between 35 and 10 Ka. Further evidence of a second carbonate-forming event or events includes the isolated outcrops of tufa and travertine of the Hudoab tufa unit in the Kuiseb Valley, dated at between 31 and 10.9 Ka [17]. Caves near Rössing Mountain contain carbonate "sinter", dated at between 42 and 23 Ka, possibly indicating relatively humid conditions at this time [18].

2.5. Gypcrete

Surface and near-surface sediments are often cemented by gypsum and bassanite, as well as carbonate [19]. Figure 4 shows a typical cross-section from the Tumas deposit in which gypsiferous sediments (sand and gravel) form a continuous layer at about 1–2 m below the surface. The layer is overlain by unconsolidated sands and gravels related to the present-day ephemeral drainage. Elsewhere, the gypsiferous layers form small scarps where they are eroded by current drainage (see Figure 3B). Locally, the gypcrete is radioactive, containing similar uranium grades to the calcrete-hosted deposits. This type of mineralisation has minimal economic potential and has not been studied in detail.

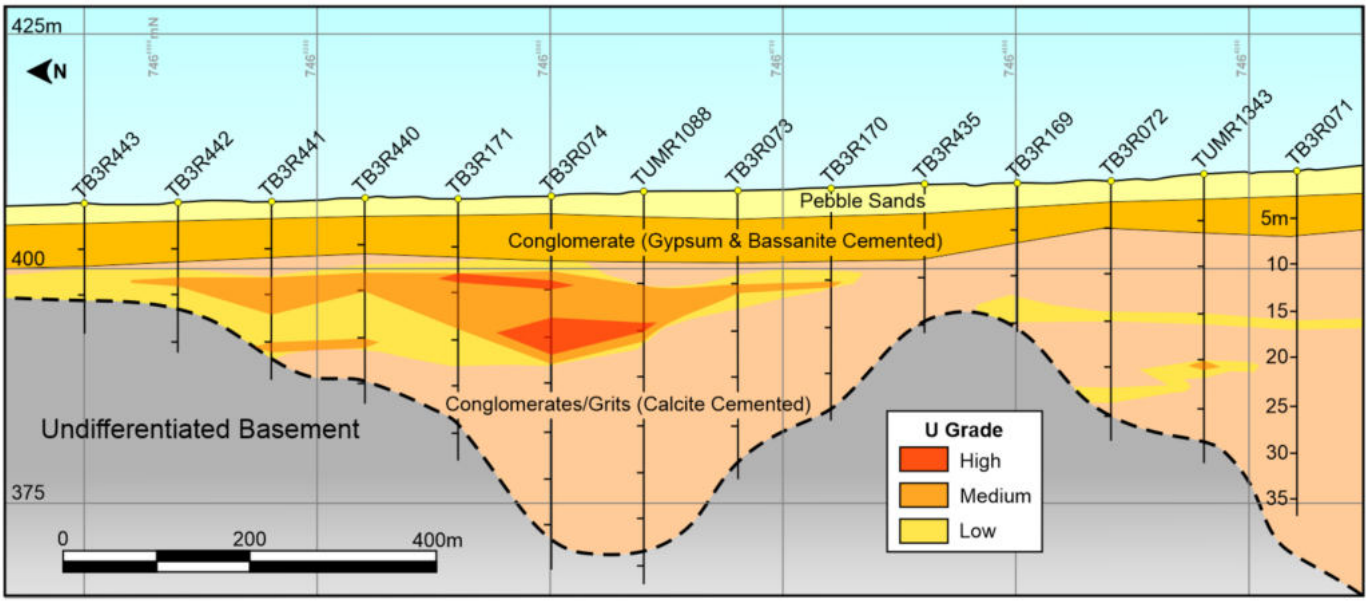

Figure 4. Typical cross section from Tumas [20].

3. The Mineralised Palaeochannels

The contemporary ephemeral drainage basins south of the Swakop River host two major palaeochannel systems and four of the larger surficial uranium deposits of the region, at Langer Heinrich, Tumas, Tubas and Aussinanis (Figure 1).

The northern palaeochannel network contains the major uranium deposits of Langer Heinrich, Tubas and Tumas, which occupy 50 and 15 km of the palaeochannel, respectively. The southern palaeochannel system contains the Aussinanis deposit, which extends over 16 km of the palaeochannel and the Namib IV deposit (also known as Aussinanis), which extends over approximately 10 km of the palaeochannel. Hence, a key feature of this style of mineralisation is its lateral extent, a feature which has important implications for genesis (see below). The depth of the palaeochannels (below surface) increases from a few metres in the east to over 100 m at the western end of the Tumas palaeochannel.

The geology of the Langer Heinrich Valley is shown in Figures 5 and 6. Unusually for the district, palaeochannel sediments (mainly carbonate-cemented conglomerates and sands of the Langer Heinrich Formation) outcrop. A prominent scarp, formed by a carbonate-cemented conglomerate to the east of the Langer Heinrich deposits (Figures 3A and 5), is a probable lateral equivalent of the Kamberg Calcrete of the Kuiseb Valley. This would

mean that the Langer Heinrich Formation is a likely lateral equivalent of the Miocene Karpfenkliff Conglomerate. The exposure of these palaeochannel sediments is the result of substantial erosion caused by the incision of the present-day Gawib ephemeral drainage (Figures 3A and 5) [15,21]. It was this incision and consequent exposure of the deeper levels of the palaeochannel that facilitated the discovery of the deposits using airborne radiometric surveys [15].

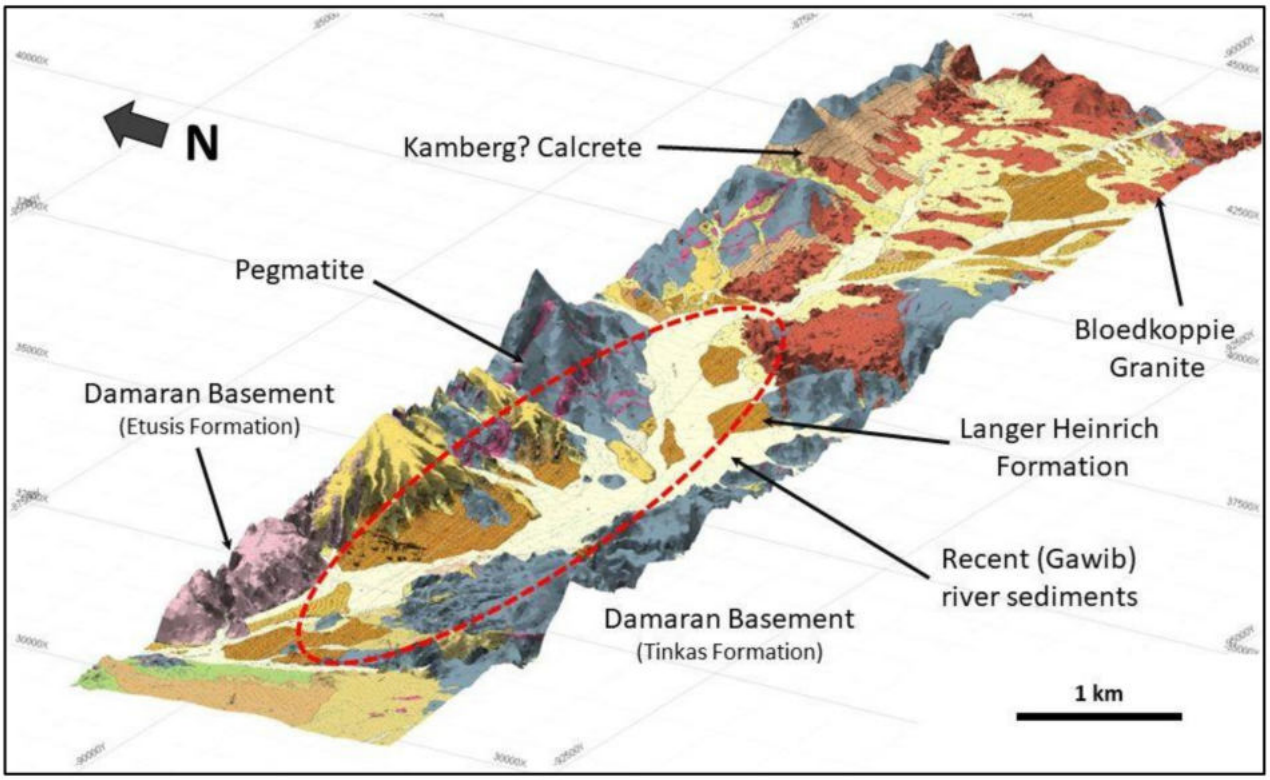

Figure 5. Geology of the Langer Heinrich Valley. Dashed red line is the approximate extent of the mineralised palaeochannel. Geology after [21]. Note ten times vertical exaggeration.

The palaeochannel fill is the dominant host to uranium mineralisation, typically a weakly stratified and poorly sorted polymict conglomerate, with clasts up to 20 cm, as well as sand-dominant layers (Figure 7A,B). Clay-rich layers are rare. Bedding can be correlated only for short distances, indicating transient high energy flows, such as flash floods typical of desert climates [22,23]. The angular habit of detrital feldspar suggests deposition close to the source [15,22]. Clasts within the mineralised conglomerates usually include abundant monomineralic black quartz, which is very probably derived from leucogranite pegmatites.

The conglomerate and sand are cemented to varying degrees by calcite (and sometimes dolomite), clay (illite, smectite, palygorskite, sepiolite etc—see below) and, rarely, cryptocrystalline silica The degree of carbonate cementation varies substantially from none to over 50% calcite. There is no correlation, however, between uranium grade and calcite abundance either at the deposit scale or in thin sections. Indeed, all palaeochannels are cemented to various degrees by carbonate minerals and clays, but the occurrence of uranium mineralisation is much more restricted. There is little or no published information on the distribution of carbonate cement within palaeochannels, but the author's observations at Tumas are that the most intense cementation typically occurs in the central portion (of a vertical section), persisting upwards to within a few metres of the surface.

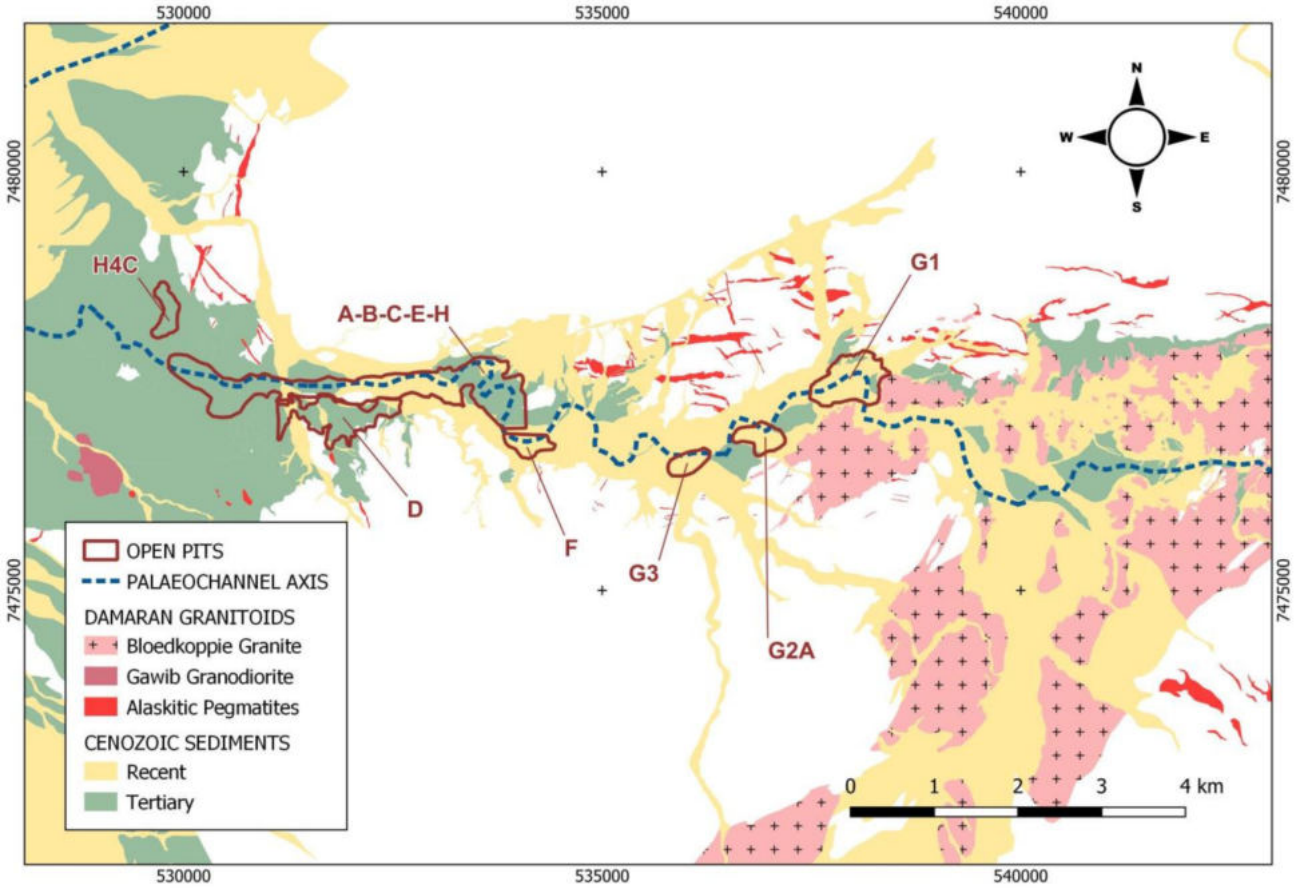

Figure 6. Simplified geological map of the Langer Heinrich area (after [21]). Recent sediments are related to the present day Gawib ephemeral drainage (see Figure 3A). White areas are outcropping Damaran metamorphic rocks, notably the schist of the Tinkas Formation. Letters refer to open pit designation.

In some parts of the palaeochannels, notably at Tubas, the dominant conglomerate/sand unit is overlain by a distinctive red sand unit. The red sand is poorly consolidated, coarse and rusty red in colour and of probable aeolian origin. This material hosts the Tubas Red Sand mineralisation. Relatively thin sandstone layers occur with the Karpfenkliff Conglomerate, but the most likely correlative of the Tubas Red Sand is the cross-bedded aeolian sand unit of the Pleistocene Oswater Conglomerate, which can reach thicknesses of 14 m [14].

A thin veneer of sediment related to contemporary ephemeral drainage, such as the Gawib and sheet wash, overlies the calcretised conglomerate or aeolian sand at all the deposits, typically reaching a few metres in thickness. This material often obscures the courses of the palaeochannels and suppresses the radiometric response of the mineralisation. At Tumas, this surficial layer overlies a gypsum–bassanite rich layer (Figure 3).

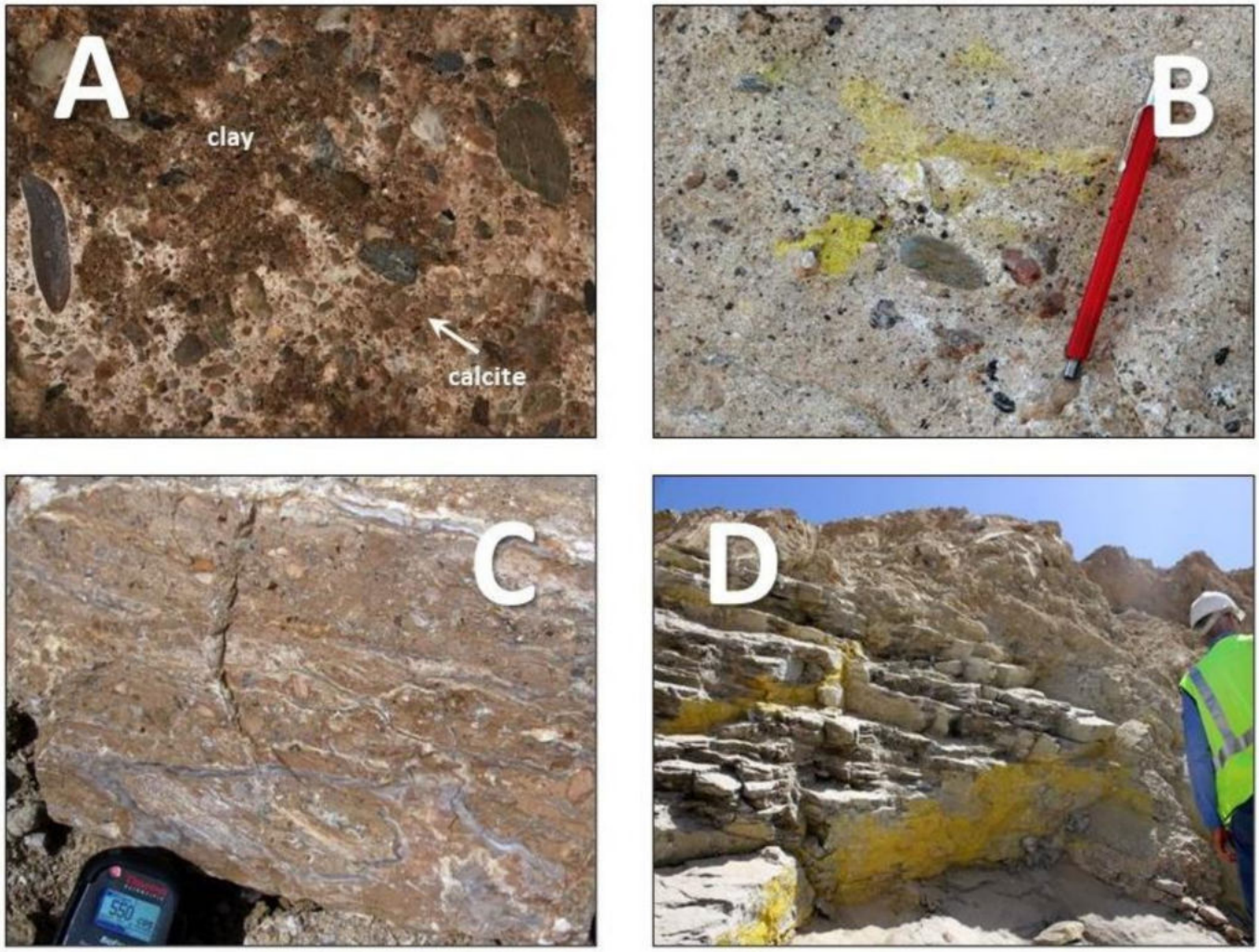

Figure 7. (**A**)—carbonate-cemented conglomerate from Tumas. Note the irregular distribution of pale calcite-cemented areas. The dominant cement is noted. (**B**)—Mineralised and calcite-cemented polymictic conglomerate from Langer Heinrich. Yellow colour is carnotite. Note the erratic distribution of the carnotite. (**C**)—Silicified conglomerate, Trekoppje open pit. (**D**)—Carnotite crusting sub-vertical fractures in schist of Tinkas formation at Langer Heinrich.

4. Uranium Mineralisation

4.1. Geometry of Mineralisation

The uranium mineralisation of the Kuiseb Basin is relatively poorly documented, despite intense exploration during the 1970s and 1980s, and again in the years after 2000. Even the mine at Langer Heinrich has yielded relatively little public domain information. It is possible to establish, however, that mineralisation typically extends over many kilometres of the palaeochannel and is somewhat irregular in form, with a tendency to occur as quasi-tabular bodies elongated in the flow direction of the host palaeochannel (Figure 1). This simple situation is complicated by the occurrence of uranium along fractures, including fractures in the underlying basement rocks. A significant but unquantified amount of uranium occurs in underlying basement rocks. This included, for example, carnotite-rich seams along open fractures in the schist of the Tinkas Formation at Langer Heinrich (Figure 7D).

4.2. Mineralogy & Paragenesis

The main ore mineral is considered to be the vanadate hydrate carnotite [$K(UO_2)(VO_4)_2.1$-$3H_2O$]; however, there have been few published studies focusing on uranium mineralisation

using modern mineralogical tools. Tyuyamunite [$Ca(UO_2)_2(VO_4)_2.7\text{-}10H_2O$] has been described at Langer Heinrich and appears to be at least as abundant as carnotite in the studied samples [24]. Carnotite and tyuyamunite occur disseminated in the host sand and conglomerates, and coating clasts and fractures (Figure 7B and Figure 9A,B).

Gangue minerals include detrital quartz, feldspar, mica, magnetite, ilmenite, titanite, zoisite and apatite [15,22]. This assemblage is consistent with derivation from a predominantly granitic source region. Post-depositional minerals are dominated by interstitial carbonate, chiefly calcite, and clays [21,22,24]. Some calcite, however, is found as rounded clasts (as in the Oswater conglomerate) suggesting the periodic emergence and erosion of carbonate-cemented rocks. Dolomite is apparently uncommon, but has been described at Langer Heinrich [21,22]. Clay minerals include palygorskite, vermiculite, sepiolite, illite, smectite and kaolinite [21,24] (Figure 8). Amorphous silica has been described at Langer Heinrich, but its abundance and distribution is poorly understood and also occurs in minor amounts at Trekkopje (Figure 7C) [21].

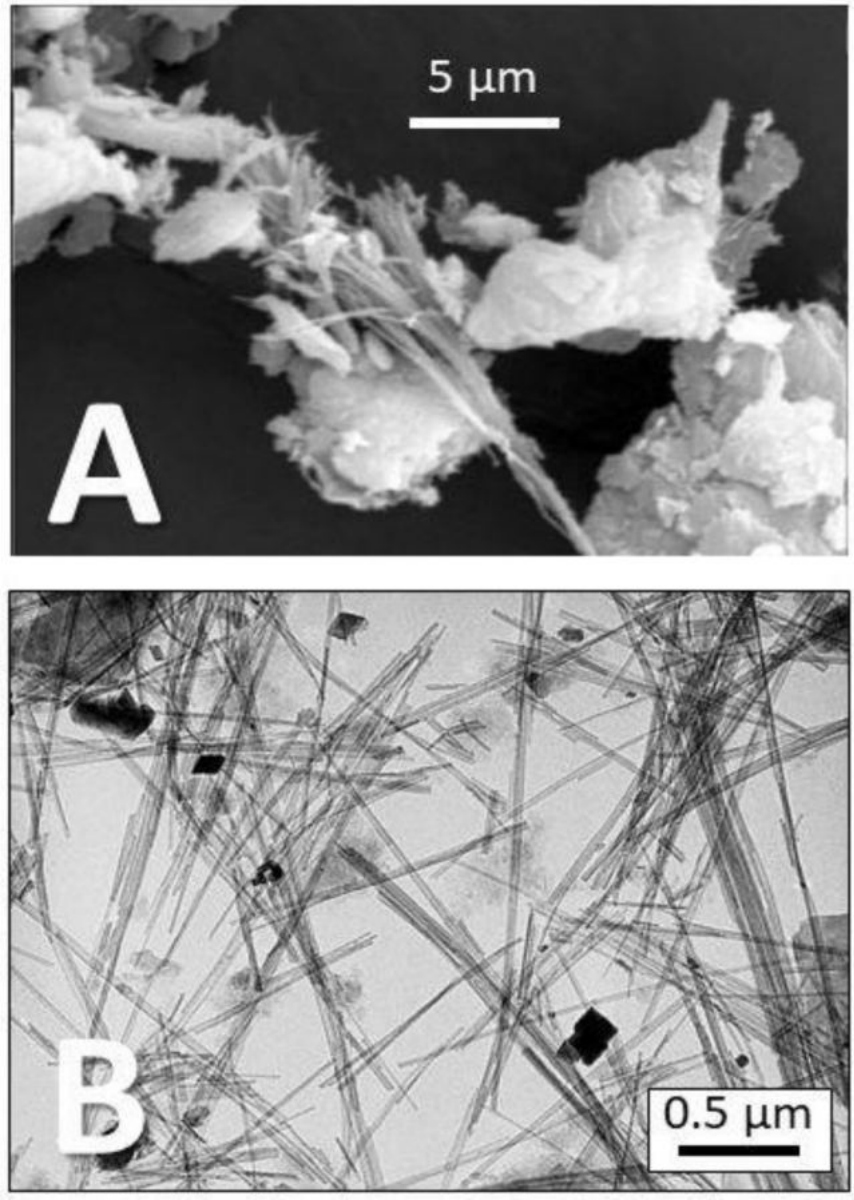

Figure 8. Interstitial clay minerals. (**A**) Back-scattered electron image of fibrous palygorskite from Langer Heinrich. Platy clay mineral not identified [21]. (**B**) TEM image of vermiculite, Langer Heinrich. Black phase unidentified [24].

The paragenesis of uranium deposition at the Tumas deposit Is illustrated in Figure 9A,B. Most carnotite is associated with Mg-rich silicates that enclose irregular calcite. The calcite is frequently heavily fractured and has a serrated contact with the clay matrix minerals. Occasional inclusions of carnotite can be observed within the calcite as in Figure 9B; however, in these cases, carnotite is almost always related to fractures in the calcite, confirming that it was introduced after formation of the calcite. Recent studies at Langer Heinrich also suggest that uranium mineralisation is paragenetically later than calcite cement, and is associated with the magnesian clay palygorskite, amorphous Mg silicate and dolomite (Figure 9C,D) [21,25].

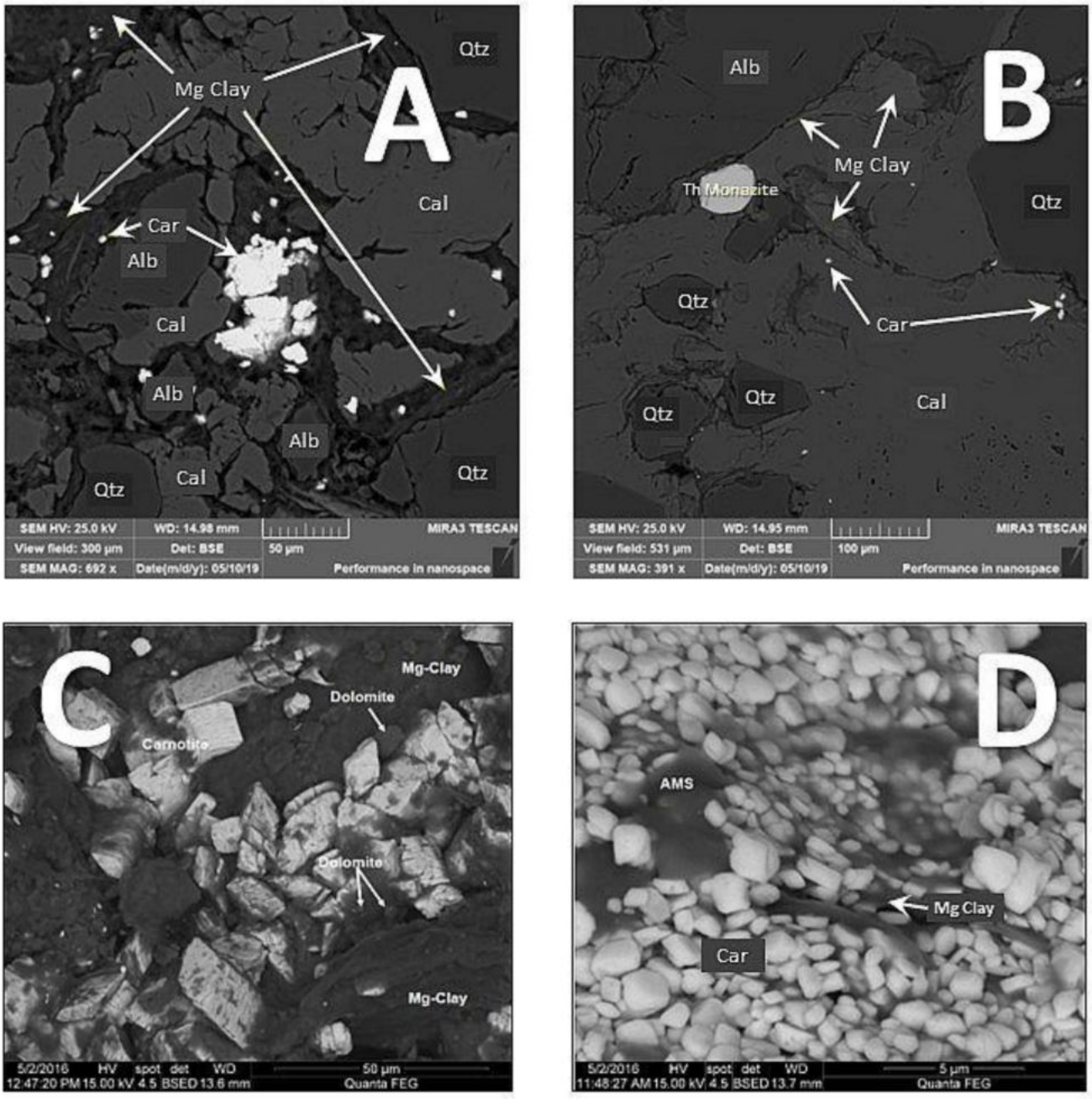

Figure 9. Back-scattered electron images showing the relationship of carnotite to detrital grains and cements. (**A**,**B**) Association of carnotite (light grey, Car) with authigenic Mg-Al silicates (Mg-Clay) and calcite (Cal). Detrital quartz (Qtz) fully enclosed in calcite cement. In addition, albite (Alb); Tumas. (**C**,**D**) Association of carnotite with dolomite, crystalline Mg silicate (Mg-Clay) and amorphous Mg silicate (AMS); Langer Heinrich [25].

4.3. Absolute Age of Uranium Deposition

The absolute age or ages of uranium deposition remain uncertain. There has been one attempt to date the Langer Heinrich deposit using an ion microprobe. Dating was carried out on grains which were found to be mixtures of the carnotite and tyuyamunite endmembers [24]. This resulted in a U-Th age of 68 ± 2 Ka [24], i.e., the Pleistocene. The authors noted the need to analyse additional samples to validate this result.

5. Discussion: The Surficial Uranium Mineral System

5.1. Architecture

The significance of terrain architecture in mineral systems analysis is that it establishes fundamental controls on the distribution of high permeability sites within the crust. Mineral systems analysis typically considers the structural control of hydrothermal mineral deposits, but the distribution of permeability is also a crucial factor in the development of surficial uranium deposits. Existing genetic models for surficial uranium posit that uranium was introduced to its depositional sites in groundwater moving downstream within palaeochannel aquifers [2,26–29]. Hence, understanding the evolution of permeability and porosity within the palaeochannels is crucial to understanding deposit genesis.

A relatively wet climate was required to scour the Damaran orogen and produce the system of palaeochannels, the substantial remnants of which we can map today. A shift to a more arid climate and a reduction in the volume and velocity of water flowing down the palaeodrainage would have induced the precipitation of carbonate, probably via evaporation (evapo-transpiration) from slow-moving groundwater [9]. Thus, climate change is an essential element of the Mineral Systems model, but the temporal relationship between uranium mineralisation and the many fluctuations of Cenozoic climate in Namibia remain poorly resolved.

The paragenetic relationship of uranium phases to calcite indicates that the cementation of the palaeochannels was well advanced prior to most uranium deposition. Much, if not all, the uranium post-dated calcite cementation. It is important to emphasise that carbonate cementation is extremely widespread, whereas the occurrence of economic levels of uranium is much less extensive.

The intensity of carbonate cementation might be expected to influence both porosity and permeability within the palaeochannels. Basement lithologies at the Trekoppje deposit have measured porosity between 1.8 and 4.2%, whereas carbonate-cemented conglomerates have porosities ranging from 10 to 30% [30]. There is a negative correlation between porosity and carbonate content in the conglomerates (Figure 10), while porosity does not correlate with uranium content [30]. The potential importance of fractures to providing porosity and permeability has not been considered, despite the fact that fractures in basement rocks clearly were the locus of uranium precipitation. Indeed, carnotite fracture coatings have also been observed by the author in core samples of carbonate-cemented conglomerates, although these appear to be relatively uncommon.

The transmissivity and hydraulic conductivity (K) of part of the Tumas palaeodrainage were measured at 1–341 m^2/day and 0.1–17 m/day, respectively, using standard pump tests [31]. To provide some perspective, the in situ recovery of uranium in sandstone aquifers ("roll-front" type deposits) generally requires K > 0.1 m/day and porosity in excess of 15% [32]. Thus, at least parts of the palaeochannels can be regarded as having good porosity and permeability. More research is required to better understand the hydrology of the palaeochannels. It seems likely that calcite cementation reduced porosity and probably permeability. The upshot of this would have been to channel groundwater flow into the deeper, less well-cemented parts of the palaeochannels.

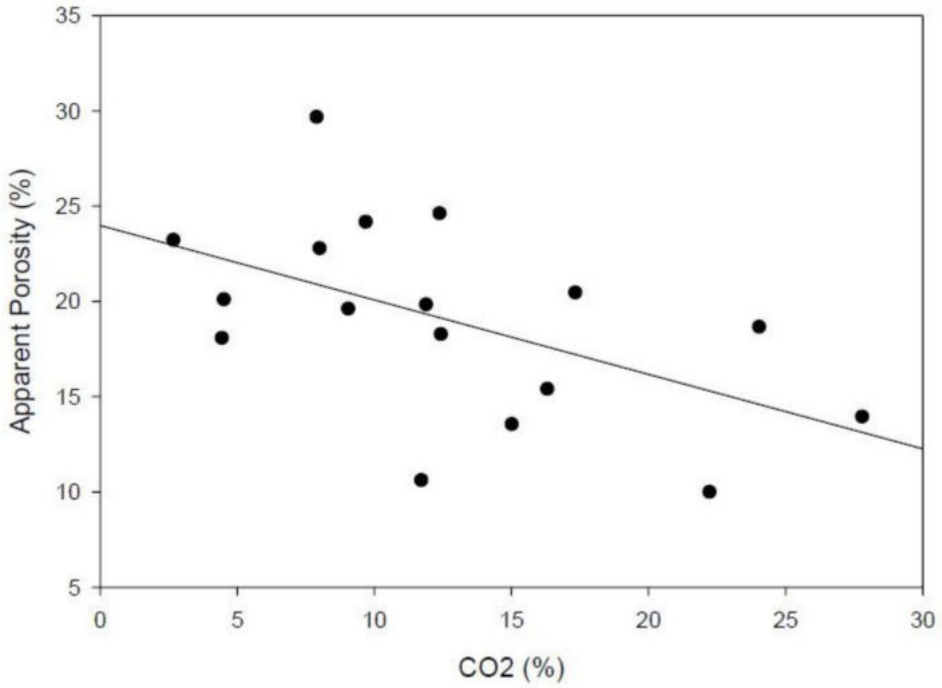

Figure 10. Relationship between measured porosity and carbonate (measured CO_2) content in conglomerates of the Trekoppje palaeochannel [30].

5.2. Source of Uranium & Vanadium

The source of uranium in these deposits is usually regarded as granitic rocks [22]. It has been suggested that uranium at Langer Heinrich was sourced from the Bloedkoppie Granite, which outcrops immediately upstream (Figure 5) and which apparently has a higher mean and median uranium content, compared to the other granitic intrusions (Table 2) [15,22,33]. Uranium in the Tumas palaeochannel is very unlikely to have been sourced from the Bloedkoppie granite (Figures 1 and 11). Recent drilling shows that the Tumas palaeochannel extends at least as far east as the Donkerhoek batholith. Indeed, the large Donkerhoek batholith is a plausible source for all the deposits south of the Swakop River, based on the fact that most of the uraniferous palaeodrainages apparently emanate from this batholith (Figure 11). Conversely, samples of the batholith reveal relatively low uranium content (Table 2).

Table 2. Mean and median abundance of U, Th and V in various granites of the Erongo region.

	U ppm			Th ppm			V ppm		
Intrusion	**#**	**Mean**	**Median**	**#**	**Mean**	**Median**	**#**	**Mean**	**Median**
Bloedkoppie	16	15	14	18	31	31	10	4	4
Bloedkoppie Pegmatite [34]	25	25		25	30				
Bloedkoppie Granite [34]	33	9		33	33				
Donkerhoek	19	3	2	38	13	11	38	20	17
Gawib	26	5	5	26	21	19	23	31	26
Vogelfederberg	12	8	4	12	54	37	12	61	48
Gray	62	15	5	63	56	28	21	49	35
Red	19	5	4	19	70	70	11	23	16
Salem	2	8	8	15	25	24	6	45	44

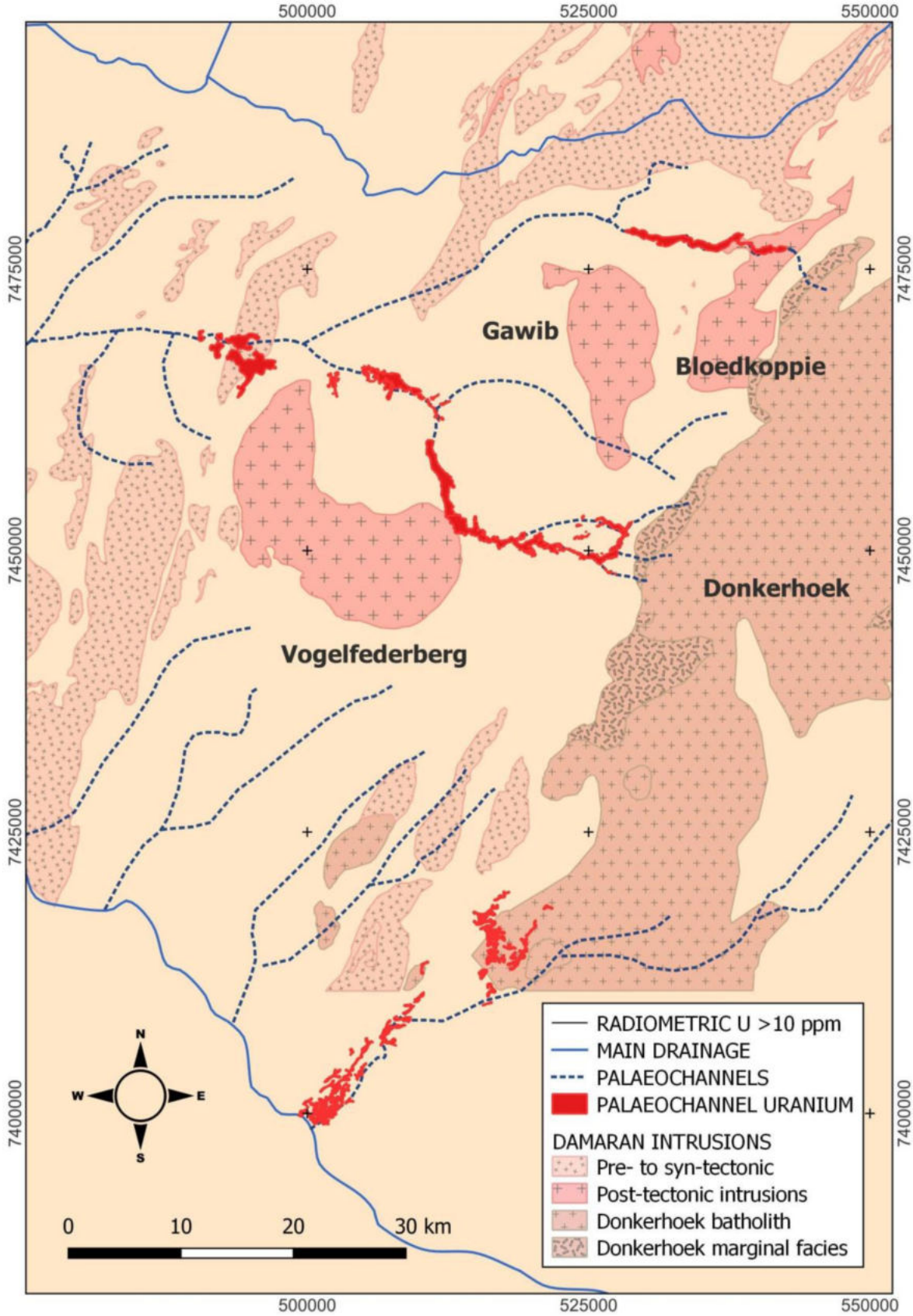

Figure 11. Simplified geological map showing the distribution of felsic intrusions north of the Kuiseb Valley.

A study of the U and Th content of the Bloedkoppie Granite, and the pegmatites that intruded it, found that the pegmatites have nearly three times the uranium content of the granite [34]. Thus, the pegmatites could be a source of more uranium than the host, but this would also depend on the relative abundance of the pegmatites within the palaeochannel catchment area. The abundance of black quartz clasts in sediments of the Langer Heinrich and Tumas palaeochannels is indicative that a significant portion of the palaeochannel sediment is derived from pegmatite, the only known source of black quartz in the region. Indeed, the Langer Heinrich open pits correspond in part to where mapped pegmatites underlie the palaeochannel (Figure 6), which adds weight to the concept that pegmatites are the principal source of uranium.

Some genetic models require separate sources of uranium and vanadium based on the assumption that significant quantities of uranium and vanadium could not be carried in the same groundwater. The geochemical modelling of contemporary groundwaters, discussed in the next section, shows that this is not necessarily the case [35]. In any case, it should be noted that many potential source granites also have much more V than U (Table 2).

5.3. Transport

It is generally assumed that uranium was introduced into its depositional site and dissolved in groundwater moving at depth through palaeochannel aquifers [2,15,23,26,36,37], probably as carbonate complexes [35]. Today, much of the hyperarid Erongo area receives <100 mm of rainfall annually. The Kuiseb River flows, on average, for only 16 days each year, with water reaching the Atlantic ocean only on rare occasions [38]. It is likely that much of the rainfall evaporates before reaching the Kuiseb and there are a few small active playas, such as Tsondab Vlei and Zebra Pan [39]. Nevertheless, the palaeochannels are charged with groundwater, as is amply evidenced by drilling [30,33,40].

Present day groundwaters from the Trekkopje deposit have uranium contents ranging from 0.1 to 0.5 mg/L, pH between 6.5 and 7.5 and eH between −50 and +150 mV; these are saturated with respect to carnotite. Therefore, these waters may be representative of mineralising groundwater [30,41]. Unfortunately, the total dissolved solids (TDS), carbonate and anion content of these samples were not analysed, so it is not possible to comment on likely uranium speciation.

Groundwaters recovered from boreholes at the Tubas deposit have a salinity (TDS) close to that of seawater, ranging from 0.7 to 4.2% and a pH range of 7.3 to 8.0; however, unlike Trekkopje, uranium was not detected [40]. The near seawater salinity may indicate that the Tubas palaeochannel was once charged with seawater. Groundwaters from the Langer Heinrich mine have a pH range from 6.9 to 7.2, a TDS ranging from 0.6 to 1.6 mg/L, and a very low uranium concentration (<180 µg/L) [33]. The V concentration in the Langer Heinrich groundwater greatly exceeds the U content, and ranges between 50 to 340 µg/L. Langer Heinrich and Tumas groundwaters are undersaturated with respect to carnotite and, therefore, are probably poor analogues for the mineralising fluids.

Many analysed groundwaters in the Erongo district have relatively high conductivity, due to high chloride content. This is reflected in airborne and ground electromagnetic (EM) surveys, which effectively map the extent of these brines and make EM a valuable exploration tool [20]. It is noteworthy that a reduced EM response can often be observed in the headwaters of palaeochannels, which can be interpreted to be the result of periodic incursion of, and dilution by, rainwater.

There has been little consideration as to whether any uranium was introduced in solid form, i.e., as detrital clasts during initial sedimentation of the palaeochannels. The amount of uranium contained in detrital phases within the palaeochannels (if any) is completely unknown. At the Beverley and Bigryli sandstone-hosted deposits in Australia, the dissolution and reprecipitation of uranium in detrital phases contributed significantly to uranium endowment [42,43]. Mining and exploration geologists in the Erongo district have noted an apparent association between the occurrence of higher uranium grades and abundant black quartz, probably derived from pegmatite. This raises the possibility

that uranium-rich phases, derived from pegmatite, were introduced as clasts during the initial stages of sedimentation of the palaeochannels; uranium was subsequently dissolved and reprecipitated more or less in situ. Indeed, the black quartz itself may be a source of uranium, as suggested by various uranium phases included in black quartz from the sub-economic Iguana alaskite-type deposit [44].

5.4. Deposition

Published genetic models for surficial uranium deposits in general posit a range of chemical depositional mechanisms. These include the mixing of U and V-rich groundwaters, pH change, evaporation, a local increase in K activity, a change in the fCO_2, the dissociation of uranyl carbonate complexes, and redox-controlled precipitation [22,23,29,30,37,41,45].

Evaporation is clearly an important process in the formation of Australian surficial uranium deposits, which typically occur in active salt lakes [2,46]. While there are some minor salt pans in the Erongo district [39,47], these do not have any spatial association with uranium deposits. Palaeo-evaporitic facies occur within the Tsondab Sandstone, but the tentative stratigraphic correlation of the palaeochannel filled with younger rocks would indicate that these evaporites predate the formation of the palaeochannel fill.

The role of evaporation in forming surficial uranium deposits in Texas was modelled using the USGS software PHREEQC and current groundwater compositions [35]. This modelling found that most modelled groundwaters precipitated calcite upon evaporation. Carnotite precipitation, however, was predicted in relatively few groundwaters and was dependent upon the major ion composition of the groundwater, specifically the ratio of Ca^{2+} to carbonate species (alkalinity) [35]. Evaporation concentrates uranium and removes CO_3^{2-} from the solution by precipitating calcite and/or dolomite. The removal of the carbonate ion from the solution, and the resultant decrease in the activity of CO_3^{2-} also decreases the activity of uranyl carbonate complexes and can lead to the precipitation of carnotite [35]. The process of evaporation may drive several other chemical changes cited as depositional mechanisms above, including pH change, a change in the fCO_2 and the dissociation of uranyl carbonate complexes. The modelling incidentally demonstrated that U and V can both be carried in natural groundwaters, meaning that the mixing of a U-rich and a V-rich fluid is not required to saturate a groundwater in uranyl vanadates [35].

The association of carnotite with Mg-rich clay minerals and dolomite at Langer Heinrich (Figure 9C,D) suggests that deposition was from a groundwater that was much richer in Mg than that in equilibrium with early calcite cement [25]. Similar mineralogy and paragenesis in the deposits of Western Australia were interpreted as the result of the "desiccation of shallow groundwater aquifers through progressive aridification" [2]. Early calcite may have played an indirect role in the formation of uranium deposits by buffering pH in the near neutral range, since the transport of uranium (as carbonate complexes) requires a neutral to alkaline pH [2].

A critical question, and one of prime importance for exploration, concerns the factors that localized uranium deposition. It has been suggested that constrictions in the palaeochannels, for example resistant dykes forming ridges perpendicular to the palaeochannel axis, lead to uranium precipitation by "ponding" groundwaters and forcing groundwater upwards towards the zone of evaporation [36]. This hypothesis seems implausible given that uranium mineralisation extends over 50 km of the Tumas palaeochannel. While considerable irregularity in the palaeochannel floor has been identified by drilling, there does not appear to be any constrictions of sufficient magnitude to cause the stagnation of groundwater flow for 50 km upstream.

Redox-controlled uranium deposition is unlikely given the absence of evidence of redox "fronts", such as those encountered in roll-front type deposits. Neither is there evidence of any relationship between mineralisation and vertical changes in redox. Furthermore, uranium in surficial deposits occurs in the oxidised 6+ state (i.e., in carnotite and tyuyamunite), rather than the reduced 4+ state.

5.5. Preservation

All known examples of surficial uranium deposits are Cenozoic in age. This is no doubt a reflection of the ease with which the mineralisation can be eroded and dispersed downstream and eventually transferred into the ocean, as at Langer Heinrich. This type of deposit, therefore, has a low preservation potential.

6. Conclusions

Since the Mineral Systems Approach considers the origin of deposits in the framework of large-scale processes from the perspective of source, fluids, transport, and trap, it has been clearly demonstrated herein that a definitive mineral systems model for surficial uranium deposits of the Erongo district requires much further research. It is possible, however, to discern an intimate linkage between uranium mineralisation and changing climate. The massive erosion of the Damaran orogen during the Cretaceous and early Cenozoic resulted in a land surface incised by a network of immature drainages. Rainfall during the early development of these drainages must have been substantial, in order to drive the necessary processes of erosion and material transport. Aridification would have resulted in filling of the drainage by sediment derived mainly from granites (sensu lato) and uraniferous pegmatites.

It is not clear what proportion of the uranium was transported in solution from source regions in the headwaters of the palaeochannels and what portion, if any, was derived from the dissolution and reprecipitation of local accumulations of clasts derived from the same source regions.

With aridification, the flow regime would have transitioned to ephemeral surface flows and a low velocity groundwater flow within the palaeochannel aquifers. As the water flow velocity continued to decline, the evaporation or evapo-transpiration near the surface drove the widespread precipitation of calcite in pore spaces of sand and conglomerate in the upper parts of the palaeochannels.

Uranium minerals probably precipitated in response to more extreme levels of evaporation of surface and/or groundwaters. Extreme evaporation would have driven the groundwater composition to higher Mg/Ca ratios as Ca was removed via calcite precipitation and to the dissociation of uranium carbonate complexes, as proposed by several previous studies, providing that the initial groundwater composition was suitable. The higher Mg/Ca ratios of the evaporated groundwater would have favoured the precipitation of Mg phases, such as dolomite and palygorskite.

A major shortcoming of the current Mineral System model is the lack of an adequate explanation for deposit localization. Uranium precipitation occurred over substantial lengths of the palaeochannel (50 km in the case of Tumas), which argues against fluid mixing and local barriers to flow as contributors to uranium localisation. The controls on uranium localisation and, therefore, the ability to predict further undiscovered uranium deposits, should be a focus of further research, as well as the factors that control uranium grade.

The Langer Heinrich mine provides evidence that recent active drainage has incised into the older palaeodrainage, probably resulting in the removal of some mineralisation. This illustrates that surficial deposits have a low preservation potential.

Funding: This research received no external funding.

Data Availability Statement: No new data were created or analyzed in this study. Data sharing is not applicable to this article.

Acknowledgments: The author wishes to acknowledge many discussions with former colleagues at Paladin Energy and Deep Yellow, including Ed Becker, Jean-Christophe Corbin and Dave Princep, and others too numerous to mention that have shaped the views contained herein. More recently, I acknowledge discussions with Justin Drummond. Three anonymous reviewers provided positive and constructive reviews that improved the manuscript.

Conflicts of Interest: The author declares no conflict of interest.

References

1. International Atomic Energy Agency. *Descriptive Uranium Deposit and Mineral System Models*; International Atomic Energy Agency: Vienna, Austria, 2020.
2. Drummond, J.B.R.; Kyser, T.K.; Bowell, R.R.; James, N.P.; Layton-Matthews, D. Diagenesis of paleodrainages in Lake Way and Lake Maitland, Western Australia, and the role of authigenic Mg-clays and dolomite in the genesis of channel and playa uranium deposits. *Can. Mineral.* **2021**, *59*, 947–984. [CrossRef]
3. Hagemann, S.G.; Lisitsin, V.A.; Huston, D.L. Mineral system analysis: Quo vadis. *Ore Geol. Rev.* **2016**, *76*, 504–522. [CrossRef]
4. Hronsky, J.M.A.; Groves, D.I. Science of targeting: Definition, strategies, targeting and performance measurement. *Aust. J. Earth Sci.* **2008**, *55*, 3–12. [CrossRef]
5. Wyborn, L.A.I.; Heinrich, C.A.; Jaques, A.L. Australian Proterozoic Mineral Systems: Essential Ingredients and Mappable Criteria. In Proceedings of the 1994 AusIMM Annual Conference, Darwin, Australia, 5–9 August 1994; pp. 109–115.
6. Deep Yellow Limited. Mineral Resource and Ore Reserve. Available online: https://deepyellow.com.au/projects/mineral-resource-and-ore-reserve/ (accessed on 4 January 2022).
7. Paladin Energy Limited. Langer Heinrich Mine. Available online: https://www.paladinenergy.com.au/langer-heinrich-mine/ (accessed on 4 January 2022).
8. Elevate Uranium Limited. Marenica Uranium Project. Available online: https://www.elevateuranium.com.au/namibia/marenica/ (accessed on 4 January 2022).
9. Chen, X.Y.; Lintern, M.J.; Roach, I.C. *Calcrete: Characteristics, Distribution and Use in Mineral Exploration*; CRC-LEME: Adelaide, Australia, 2002; p. 170.
10. Holwell, D. Using The Mineral Systems Approach To Increase Exploration Success. *SRK News*, 2018; p. 4.
11. Longridge, L.; Kinnaird, J.; Gibson, R.; Hawkesworth, C.; Armstrong, R. Crustal recycling in the Damara Belt, Namibia, and interaction of the Congo and Kalahari Cratons; evidence from zircon U-Pb, Hf and O isotopes. *S. Afr. J. Geol.* **2018**, *121*, 237–252. [CrossRef]
12. Jacob, R.E.; Kröner, A.; Burger, A.J. Areal extent and first U-Pb age of the Pre-Damaran Abbabis complex in the central Damara belt of South West Africa (Namibia). *Geol. Rundsch.* **1978**, *67*, 706–718. [CrossRef]
13. Ollier, C.D. Outline Geological and Geomorphological History of the Central Namib Desert. *Madoqua* **1977**, *10*, 207–212.
14. Ward, J.D. *The Cenozoic Succession in the Kuiseb Valley, Central Namib Desert*; Memoirs of the Geological Survey of South West Africa/Namibia; Geological Survey of South West Africa/Namibia: Windhoek, Namibia, 1987; Volume 9, p. 43.
15. Becker, E.; Karner, K. *Geological Setting of the Langer Heinrich Uranium Deposit, Namibia*; IAEA: Vienna, Austria, 2006; p. 10.
16. McInnes, B.I.A.; Evans, N.J.; Boni, M.; McDonald, B.J. (U–Th)/He thermochronometry of supergene base metal ores and implications for Namibian Paleoclimate. *Geochim. Cosmochim. Acta* **2006**, *70*, A411. [CrossRef]
17. Vogel, J.C. Evidence of past climatic change in the Namib Desert. *Palaeogeogr. Palaeoclimatol. Palaeoecol.* **1989**, *70*, 355–366. [CrossRef]
18. Geyh, M.A.; Heine, K. Several distinct wet periods since 420 ka in the Namib Desert inferred from U-series dates of speleothems. *Quat. Res.* **2014**, *81*, 381–391. [CrossRef]
19. Wilkinson, M.J. *Palaeoenvironments in the Namib Desert*; University of Chicago: Chicago, IL, USA, 1990.
20. Wilde, A.R.; Corbin, J.-C.; Becker, E. New Approach to Exploring the Tumas Palaeochannel Identifying New Potential and Resources, Erongo, Namiba. In Proceedings of the Uranium 2019, Adelaide, Australia, 4–5 June 2019.
21. Trittschack, R. *Geological Identification and Mineralogical Characterisation of Palaeosurfaces and Channel Fills at the Langer Heinrich Uranium Deposit, Namibia*; Martin-Luther-University Halle-Wittenberg: Halle, Germany, 2008.
22. Hartleb, J.W.O. The Langer Heinrich uranium deposit: Southwest Africa/Namibia. *Ore Geol. Rev.* **1988**, *3*, 277–287. [CrossRef]
23. Hambleton-Jones, B.B.; Levin, M.; Wagener, G.F. Uraniferous Surficial Deposits in Southern Africa. In *Mineral Deposits of Southern Africa*; Geological Society of South Africa: Johannesburg, South Africa, 1986; pp. 2269–2287.
24. Fleurance, S.; Cuney, M.; Kinnaird, J. *Mineralogical, Geochemical and Isotopic Study of 6 Samples from the Langer Heinrich Calcrete Deposit (Namibia)*; Henry Poincare University: Johannesburg, South Africa; University of the Witswatersrand: Johannesburg, South Africa, 2011; p. 23.
25. Drummond, J. *Mineralogical Studies on Langer Heinrich*; Queens University: Kingston, ON, Canada, 2022.
26. Chudasama, B.; Porwal, A.; González-Álvarez, I.; Thakur, S.; Wilde, A.; Kreuzer, O.P. Calcrete-hosted surficial uranium systems in Western Australia: Prospectivity modeling and quantitative estimates of resources. Part 1—Origin of calcrete uranium deposits in surficial environments: A review. *Ore Geol. Rev.* **2018**, *102*, 906–936. [CrossRef]
27. Arakel, A.V.; McConchie, D. Classification and genesis of calcrete and gypsite lithofacies in paleodrainage systems of inland Australia and their relationship to carnotite mineralization. *J. Sediment. Petrol.* **1982**, *52*, 1149–1170. [CrossRef]
28. Hou, B.; Keeling, J.; Li, Z. Paleovalley-related uranium deposits in Australia and China: A review of geological and exploration models and methods. *Ore Geol. Rev.* **2017**, *88*, 201–234. [CrossRef]
29. Mann, A.W.; Deutscher, R.L. Genesis principles for the precipitation of carnotite in calcrete drainages in Western Australia. *Econ. Geol. Bull. Soc. Econ. Geol.* **1978**, *73*, 1724–1737. [CrossRef]
30. Youlton, B. *Controls on Uranium Mineralization at the Klein Trekkopje Prospect, Namibia*; University of the Witwatersrand: Johannesburg, South Africa, 2008.
31. Bittner, A.; Gustavo, E. *Groundwater Baseline Study of Tumas Palaeochannel*; SLR: Windhoek, Namibia, 2020; p. 61.

32. Myers, E.; Maerten, H.; Nicolai, J.; Zauner, M. Applicability of permeability enhancement for in-situ recovery. In Proceedings of the Alta 2020, Online, 9–27 November 2020; p. 1.
33. Lilende, A. *The Source of Uranium and Vanadium at the Langer Heinrich and Klein Trekkopje Uranium Deposits—Genesis and Controlling Factors for Uranium Mineralisation*; University of Namibia: Namibia, South Africa, 2012.
34. Kamona, F. *Concentration of U and Th in the Bloedkoppie Granite, Namibia*; Springer: Berlin/Heidelberg, Germany, 2011; pp. 111–118. [CrossRef]
35. Ranalli, A.J.; Yager, D.B. Use of mineral/solution equilibrium calculations to assess the potential for carnotite precipitation from groundwater in the Texas Panhandle, USA. *Appl. Geochem.* **2016**, *73*, 118–131. [CrossRef]
36. Chudasama, B.; Porwal, A.; Wilde, A.; González-Álvarez, I.; Aranha, M.; Akarapu, U.; Hirsch, M.; Becker, E. Bedrock topography modeling and calcrete-uranium prospectivity analysis of Central Erongo Region, Namibia. *Ore Geol. Rev.* **2019**, *114*, 103109. [CrossRef]
37. Hambleton-Jones, B.B. Surficial Uranium Deposits in Namibia. In *Report of the Working Group on Uranium Geology*; International Atomic Energy Agency: Vienna, Austria, 1984; pp. 205–216.
38. Stone, A.E.C.; Thomas, D.S.G.; Viles, H.A. Late Quaternary palaeohydrological changes in the northern Namib Sand Sea: New chronologies using OSL dating of interdigitated aeolian and water-lain interdune deposits. *Palaeogeogr. Palaeoclimatol. Palaeoecol.* **2010**, *288*, 35–53. [CrossRef]
39. Eckardt, F.D.; Drake, N.; Goudie, A.S.; White, K.; Viles, H. The role of playas in pedogenic gypsum crust formation in the Central Namib Desert: A theoretical model. *Earth Surf. Process. Landf.* **2001**, *26*, 1177–1193. [CrossRef]
40. Stanton, M. *Omahola Project—Groundwater Monitoring Baseline Report*; Eco Aqua: Swakopmund, Namibia, 2010; p. 50.
41. Hambleton-Jones, B.B.; Smit, M.C.B. *Calculation of the Carnotite Solubility Index. Surficial Uranium Deposits*; IAEA: Vienna, Austria, 1984; pp. 81–86.
42. Wülser, P.-A.; Brugger, J.; Foden, J.; Pfeifer, H.-R. The sandstone-hosted Beverley uranium deposit, Lake Frome basin, South Australia; mineralogy, geochemistry, and a time-constrained model for its genesis. *Econ. Geol. Bull. Soc. Econ. Geol.* **2011**, *106*, 835–867. [CrossRef]
43. Schmid, S.; Taylor, W.R.; Jordan, D.P. The Bigrlyi Tabular Sandstone-Hosted Uranium-Vanadium Deposit, Ngalia Basin, Central Australia. *Minerals* **2020**, *10*, 896. [CrossRef]
44. Wilde, A.R.; Teale, G.; Shidolo, S. Hydrothermal U-Fe-Cu Mineralisation in the Southern Central Zone of the Damara Orogen, Namibia. In Proceedings of the Geological Society of Namibia 50th Anniversary Conference, Windhoek, Namibia, 1–4 September 2019; pp. 51–52.
45. Hambleton-Jones, B.B. *The Geology and Geochemistry of Some Epigenetic Uranium Deposits Near the Swakop River, South-West Africa*; University of Pretoria: Pretoria, South Africa, 1976.
46. Guan, Q.; Mei, Y.; Etschmann, B.; Testemale, D.; Louvel, M.; Brugger, J. Yttrium complexation and hydration in chloride-rich hydrothermal fluids: A combined ab initio molecular dynamics and in situ X-ray absorption spectroscopy study. *Geochim. Cosmochim. Acta* **2020**, *281*, 168–189. [CrossRef]
47. Eckardt, F.D.; Livingstone, I.; Seely, M.; Von holdt, J. The surface geology and geomorphology around Gobabeb, Namib desert, Namibia. *Geogr. Annaler. Ser. A Phys. Geogr.* **2013**, *95*, 271–284. [CrossRef]